TEMPLATE
BUKU PROFIL PENYELIDIKAN SKIM GERAN PENYELIDIKAN
GERAN UNIVERSITI JANGKA PENDEK / GERAN DALAM UMP

DIRECT METAL LASER SINTERING TECHNOLOGY FOR THE MANUFACTURE OF FULLY POROUS FUNCTIONALLY GRADED TITANIUM ALLOY FEMORAL STEMS (FABRICATION AND DESIGNING OF FULLY POROUS FUNCTIONALLY GRADED TITANIUM ALLOY FEMORAL STEMS)

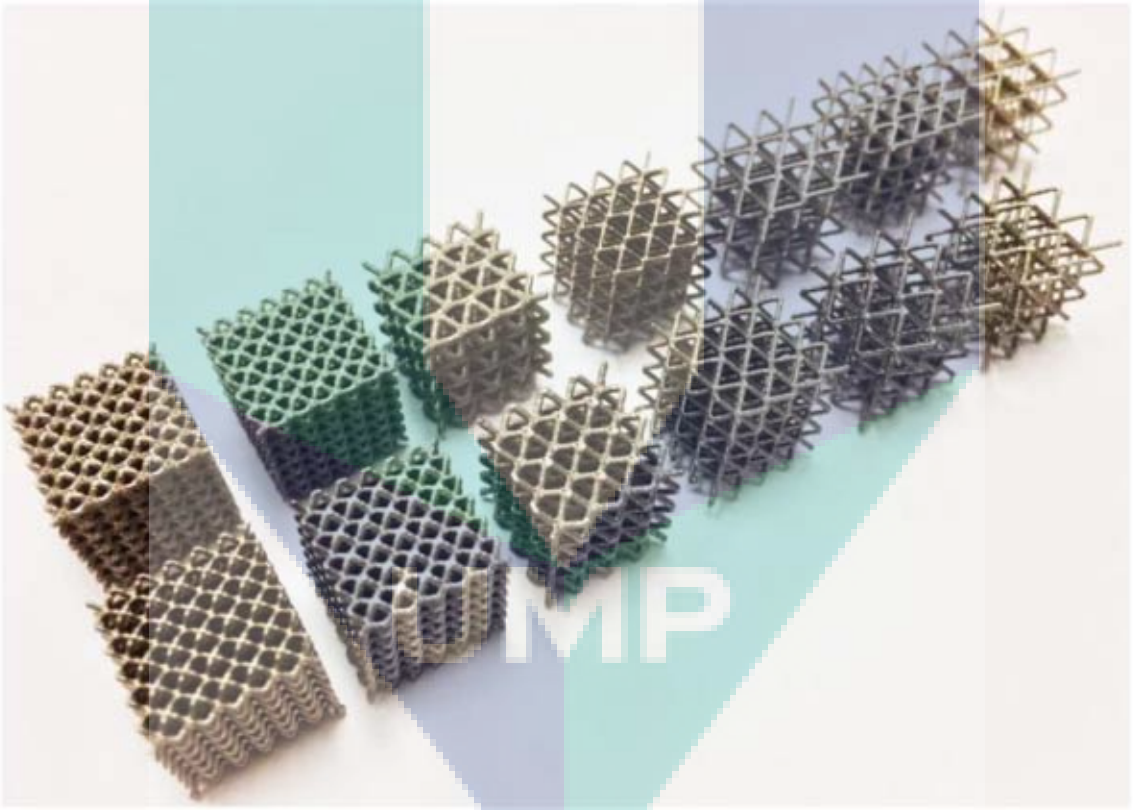

Name of Project Leader

ASSOC. PROF. IR. TS. DR. KUMARAN KADIRGAMA

Name of co-researchers

Prof.Dr.Mustafizur Rahman

Assoc.Prof.Dr.Wan Sharuzi Wan Harun

ABSTRACT (120 words)

This report investigates the properties of titanium alloy (Ti6Al4V) lattice structures fabricated via selective laser melting (SLM). Response surface method (RSM) was used to design the experiments. Four factors were selected to determine its influence on the Young's modulus and compressive strength. Detailed characterizations such as dimensional accuracy, surface roughness, microstructure analysis, and compression test were conducted and reported. The built structures have a Young's modulus ranging between 0.01 and 1.84 GPa. The statistical method was used to find the relationship between factors and Young's modulus and compressive strength. Porosity was comprehended to play a significant role in determining the Young's modulus and compressive strength. The error of the developed model was in the range of 0.5 to 1.3% compared with experimental results. Meanwhile, all the four factors found not to affect the surface roughness significantly. The statistical method recognizes the trends of the factor effect on the Young's modulus, yield stress, and surface roughness.

1. INTRODUCTION

Additive manufacturing (AM) techniques such as 3D printing and selective laser melting (SLM) is an advanced technology available at present for contemporaneous product development. Additive manufacturing is a fabrication process where 3D model data is revolved into a three-dimensional near-net functional component [1]. Additive manufacturing enables the fabrication of intricate design without any complication [2] and with minimal environmental impact [3]. This technique is known to be exceptionally suitable for low production manufacturing [4]. SLM is one of the AM techniques which develop a product through a sequential arrangement of melted metal powders layer by layer under an inert atmosphere using a scanning laser beam [5]. In the SLM method, the model is required to be designed using computer-aided design software prior to actual fabrication. According to the literature, the titanium alloy (Ti6Al4V) components produced via SLM is usually used in aerospace [6], biomedical [7], and automotive applications [8]. Titanium alloy is specifically chosen for this applications as they are highly resistant to corrosion, biocompatible [9], and have high specific strength [10, 11].

2. RESEARCH METHODOLOGY

The mechanical properties of Ti6Al4V are testified to be dependent on the arrangement of the phase constituent at a microscopic scale [21]. According to Hanzl et al. [22], Ti6AL4V does not have a fine-grained structure. Instead, they have a line and layerwise building structure which causes them to be not homogenous. As such, a relatively dense Ti6Al4V can be produced through a selection of a suitable processing parameter combination [23]. Whereas, the porous structure can be formed by controlling the SLM laser pass speed, laser power, and powder's quality [24]. SLM produces homogenous microstructure at lower temperature regardless of build size and orientation [25]. According to Kruth et al. [26], it is essential to control the thermal gradients and build near fully dense parts simultaneously. From the literature, immense interest has been shown in studying the relationship between processing microstructure and quality of the component produced by SLM techniques, primarily using Ti6Al4V. In line with the attentiveness, this article investigates the possibility of assembling cross-section structures with custom-made porosity embracing SLM process and their properties. The sample is fabricated using the EOSINT M270 adapting the laser-sintering framework

with improved parameters to acquire the full thickness of laser-sintered parts. In this work, the sample was fabricated with an open cellular structure with four controlled parameters. Ti6Al4V powder with a mean particle size of 30 µm is used in this investigation. The powder quality is imperative to lessen the substance of debasements (oxygen, hydrogen, and nitrogen), which may influence mechanical properties of laser-sintered parts. Design of experiments is used to develop the experiment table. Figure 1 shows the strut designs that were drawn using CAD software. Based on the design, their volume porosity is determined to be 70, 75, 80, 85, 90, and 95%, respectively. Total numbers of samples fabricated is 13 with 5 replications for each parameter.

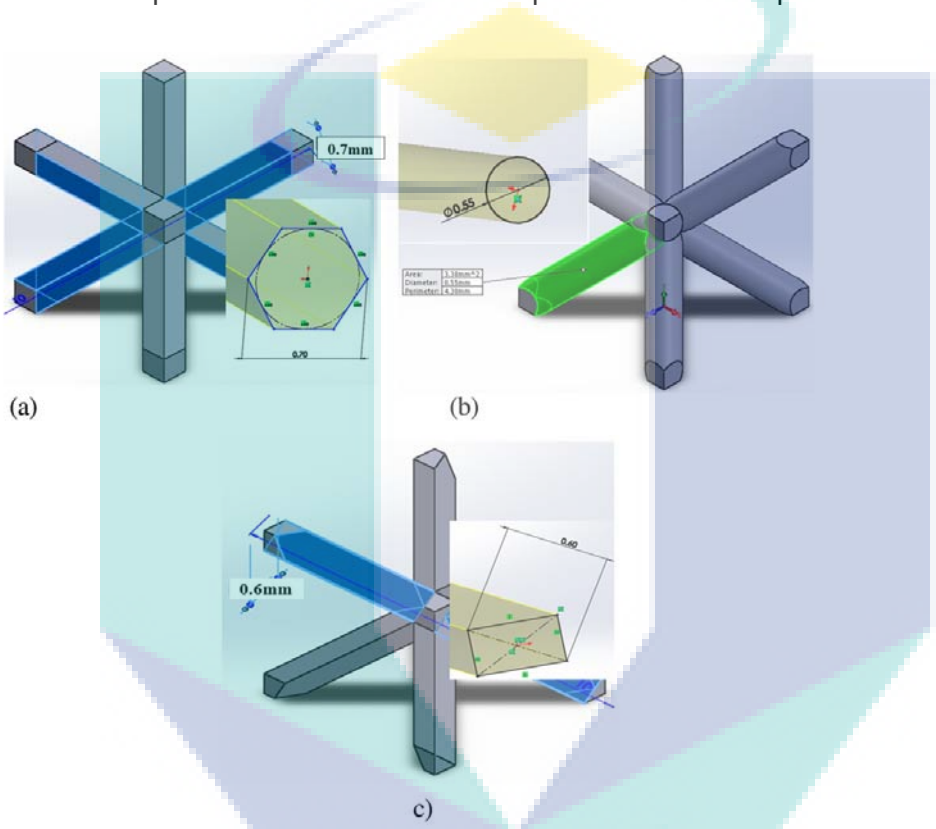

Figure 1: a) Strut 0.7 mm, hexagon; b) strut 0.55 mm, circle; c) strut 0.6 mm, square

3. LITERATURE REVIEW

At present, the research on Ti6Al4V has been focused on using them to develop sophisticated orthopedic implants [12–15]. Harrysson et al. [13] and Hazlehurst et al.[14] have utilized EBM/Ti6Al4V and SLM/CoCrMo, individually, to develop permeable and solid femoral stems.
Harrysson et al. [13] chose a rhombic dodecahedron grid structure with a cell size of 3 mm to develop the body of the permeable stem. Whereas, Hazlehurst et al. [14] develops the permeable body by choosing a cubic cross-section structure encompassed by a dense external shell. Both of this approaches have reduced the weight of stem by 44–48% and flexural stiffness by 57–60% compared with their dense counterparts. Apart from that, since Ti6Al4V is preferably fabricated using SLM, most of the research has also been concentrated on studying the mechanical properties and failure mechanism [16] of the structure develop through the SLM process. From the previously conducted

studies, it was reported that the properties of the component are ultimately reliant on the strut size and no notable shortcoming in the associating layers of the structures is observed when subjected to shearing powers. Min et al. [17] had performed the pressure weakness testing on titanium combination cell structures and witnessed the weariness quality expanded with an expanding relative thickness and cyclic tightening of the struts inside the cell structure, which is the cause for failure. Spoerke et al. [18] reported that the fatigue strength and energy absorption of titanium structures fabricated by the SLM could be enhanced by performing a warm treatment. He also proposed several regions that could be further strengthened to make equivalent load dissemination inside the structure. Morlock et al. [19] investigated the mechanical properties of an open cell CoCrMo structure with a pore size of 0.5 mm and reported the structure to have comparable mechanical properties to monetarily fabricated components using elective composites. Furthermore, his recent findings have shown that square pore CoCrMo cell structures fabricated utilizing SLM offers compressive properties similar to human bone [20]. Based on the executed literature analysis, the author noticed a lack of information available on statistical models and the influence of the processing parameters toward the mechanical properties of SLM fabricated Ti6Al4V components. Thus, this paper epitomizes the mechanical properties such as Young's modulus and yield stress of different cross-section structures made up from Ti6AL4V using SLM. The dimensional accuracy and surface roughness of the built structure were also investigated. Four processing parameter was considered in this study namely, strut size, struct shape, unit cell, and porosity. The statistical method was used to develop the mathematical model to determine the utmost influential parameters toward the responses (Young's modulus, surface roughness, and yield stress). The optimization of the parameters values to produce structure near to human bone properties is also discussed in the paper.

4. FINDINGS

In alloys with low concentrations of beta-stabilizing elements, like Ti6Al4V, the martensite has a distorted hexagonal crystal lattice [27]. Fast hardening after the connection with the laser bar prompts more prominent hardness esteem contrasted with those of mass base material, as appeared in past smaller-scale hardness tests. Besides, no grain introduction was witnessed demonstrating the SLM's ability to create parts with isotropic properties. Strut cross-sections with different porosities are shown in Figs. 10, 11, 12, and13. It is shown that the entire strut demonstrates the near fully dense struts for the as-built Ti6Al4V lattice structure, which is also consistent with the density measurements. A small number of irregular pores is observable. This micropore may be attributed to the high residual stress, gas entrapment, and keyhole effects by metal evaporation during laser scanning [2, 14]. From the optical microscopy analysis, a columnar grain oriented vertically along the built direction is observed. This columnar grain is observed to form at the slow cooling and steep temperature gradient sites due to the physical shape of strut structures.

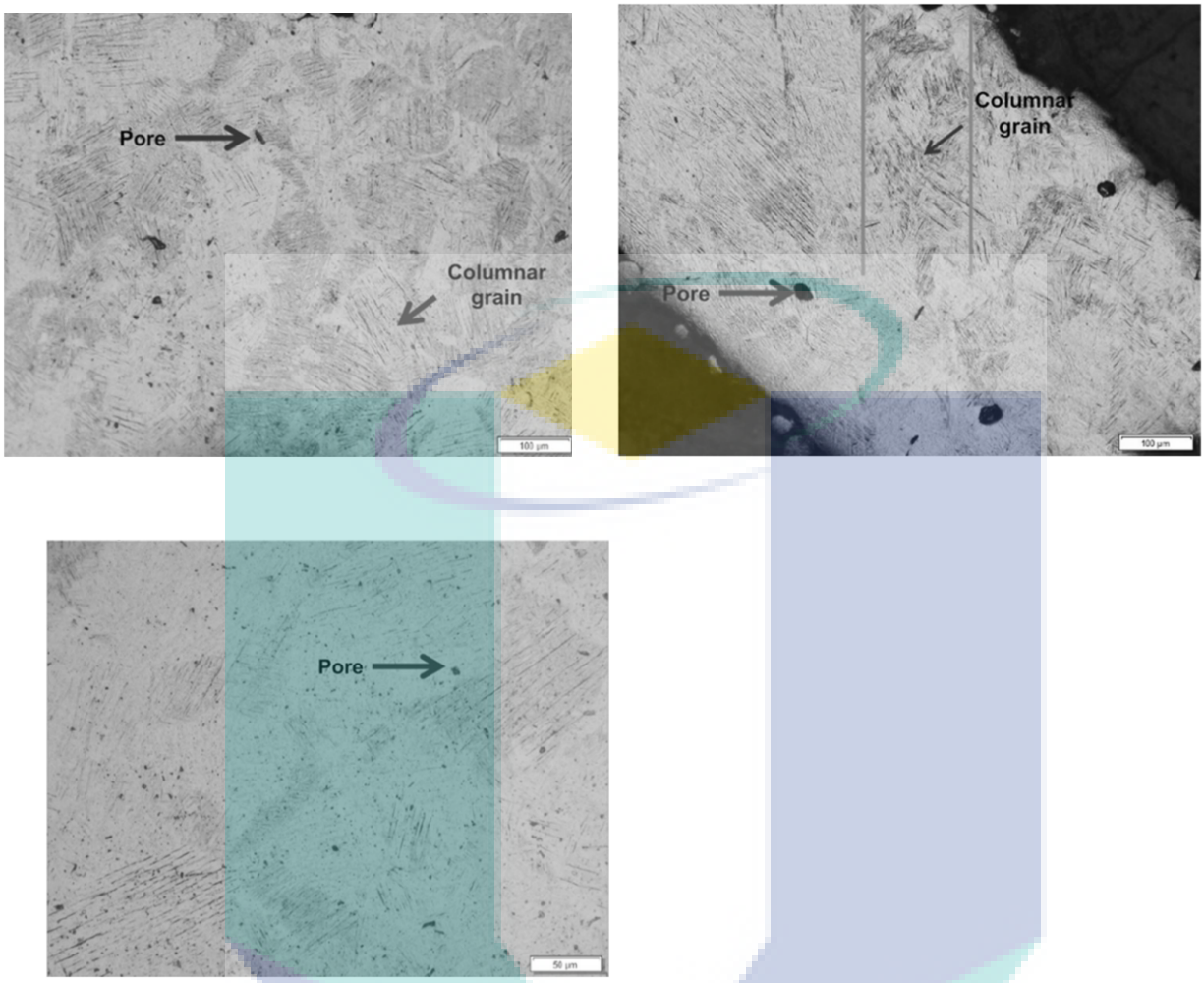

Figure 1: Porosity, 95%; magnification, ×10

It is vital to evaluate the surface roughness of the implant as rough surface promotes and upgrades the bone-embed settling and quickens the recuperating procedure as unpleasantness increases osteo-conductivitym [28]. In the wake of playing out a preparatory test on example unpleasantness, a cut off of 2.5 mm was picked by ISO 4288-2000 standard [29] to guarantee excellent reliability in Ra range for samples under examination. The experiments on surface roughness stated that Ra roughness for lattice structures ranges from 8 to 13 µm, as shown in Fig. 16. The specimens were evaluated from two sides, a top view and a side view. From the top view, hatching distance or spacing from SLM process will be surfaced, while from the side view, layer thickness was detected.

The stiffness of the open cellular structure sample will be presented in terms of Young's modulus value. The Young's modulus represents the modulus of elasticity which indicates the rigidity of the sample. From the study conducted by Nazarian et al. [30] and Rohlmann et al. [31] on the actual human femur trabecular bone, they found that Young's modulus falls between 0.32 and 0.40 GPa. The sample with cellular structures was built using the SLM250HL machine (SLM Solutions GmbH). A laser power of 100 W and a scan speed of 450 mm/s was applied to build the cellular structure sample with material densities (strut 14 density) of 95% and above. The sample was attached to the substrate plate by additional vertical struts to guarantee an easy removal of the samples

from the base plate. Wire cutting (electric discharge machining) was used to detach the samples from the substrate plate without damaging any lattice structure and to get a smooth surface for clamping the specimens during compression testing. The compression test was performed using a Shimadzu Testing System (VHS8800) with a low-rate method. The loading capacity of the machine is 100 kN. The load history was measured by a Kistler load cell 9071A. The displacement history was measured by an internal linear variable differential transformer with data filter by setting a cut-off frequency of 1000 Hz. The deformation process was also recorded by a camera within an interval of 30 s. The examples are placed on the base pressure plate which is situated at an extensive separation from the best plate toward the start of every pressure test. In any case, it ought to be noticed that the grinding impact on the uniaxial level are not very huge for crushable cell materials, because of the Poisson's proportion amid the pressure in the level area of a specimen to near zero. This quality relates to the most extreme concern that the structure can bolster before crumple. Continuous stacking brought about a plastic fall until breaking and densification. The level of softening is by all accounts more influenced by porosity. For impact energy absorption applications, stress versus strain response with little or no softening after yield is desirable [32, 33]. As shown in Fig. 10, the amount of porosity has a significant effect on the stress-strain behavior of the sample. The lower amount of porosities at 70,75, and 80% showed a higher stress which later can be translated into the higher value of Young's modulus. Higher Young's modulus means higher stiffness. The samples with a higher amount of porosity demonstrated lower value of Young's modulus which translated into lower stiffness. The summary of the Young's modulus value is shown in Table 5. Each stress-strain curve can be divided into three main phases: elastic deformation, shear deformation, and collapse. As shown in Fig. 2, all samples at different porosities demonstrated these regions evidently. However, the significant difference between the samples is the width of each region. The sample with a lower amount of porosity demonstrated more prominent region of elastic deformation and smaller region of shear deformation before collapsing. Whereas, the 16 higher porosity samples show the opposite, where they have smaller elastic region and significant shear deformation region, as shown in Figure 2.

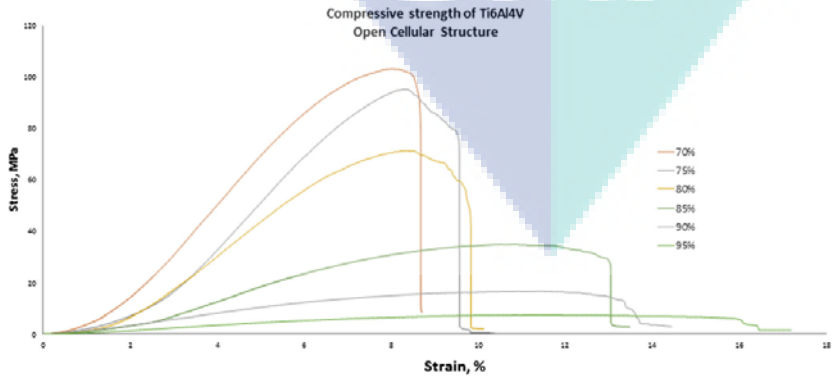

5. CONCLUSION

Ra roughness for lattice structures ranges from 8 to 13 μm for top and side views, respectively. In particular, lattice structure size was measured and their average values were reported, where volume of CT scan file sample was expanded by 2.92% from the original sample in CAD. The sample height was not considered since it is influenced by the completing operations than the building abilities of the SLM. It can be induced that deviations from display measurements are very little;notwithstanding considering every estimation, the hole is under 50 μm. The layer manufacture of the procedure prompts a specific dimensional variety at the level of the single cell.The amount of porosity has a significant effect on the behavior of the stress-strain properties of the samples. Lower amount of porosities such as 70,75, 80, and 90% showed a higher stress which later can be translated into the higher value of the Young's modulus. Higher Young's modulus means higher stiffness. On the one hand, the samples with a higher amount of porosity demonstrated the lower value of Young's modulus which translated into lower stiffness. Each stress-strain curve can be divided into three main phases: elastic deformation, shear deformation, and collapse. The main effect plot shows that lower porosity increases the Young's modulus and yield stress of the structure. Contour and surface plots show that for all the shapes, the Young's modulus increases with low porosity and struct size at 0.6 mm. An equation was developed with porosity and Young's modulus from the experimental data. The four factors do not affect the surface roughness of the structure. The trend of each factor can be known from the factorial plot. It shows that roughness is increased with increased of porosity, struct size, and unit cell. It is shown that the optimum structure parameters that are produce near to the 0.4 GPa are unit cell = 4 × 4 × 4, strut size = 0.7 mm, porosity = 91, and struct shape = H.

ACHIEVEMENT

i) Name of articles/ manuscripts/ books published

1. A comprehensive review of hydroxyapatite-based coatings adhesion on metallic biomaterials, Ceramics International, 44 (2018) 1250–1268

2. Statistical and optimize of lattice structures with selective laser melting (SLM) of Ti6AL4V material, The International Journal of Advanced Manufacturing Technology (2018) 97:495–510

3. Finite element study of functionally graded porous femoral stems incorporating body centered cubic structure, Artificial organ,

.

ii) Human Capital Development

- Rahil Izzati – Graduated 2017

REFERENCES

Zhai Y, Lados DA, LaGoy JL (2014) Additive manufacturing: making imagination the major limitation. JOM 66(5):808–816

2. I. Gibson, D. W. Rosen, and B. Stucker 2010 Additive manufacturing technologies. Springer

3. Drizo A, Pegna J (2006) Environmental impacts of rapid prototyping: an overview of research to date. Rapid Prototyp J 12 (2):64–71

4. Cooper DE, Stanford M, Kibble KA, Gibbons GJ (2012) Additive manufacturing for product improvement at red bull technology. Mater Des 41:226–230

5. Kruth J-P, Froyen L, Van Vaerenbergh J, Mercelis P, Rombouts M,Lauwers B (2004) Selective laser melting of iron-based powder. JMater Process Technol 149(1):616–622

6. Brandt M, Sun SJ, Leary M, Feih S, Elambasseril J, Liu QC (2013)High-value SLM Aerospace components: from design to manufacture. Adv Mater Res 633:135–147 7. Parthasarathy J, Starly B, Raman S (2011) A design for the additive manufacture of functionally graded porous structures with tailored mechanical properties for biomedical applications. J Manuf Process 13(2):160–170

8. Cooper D, Thornby J, Blundell N, Henrys R, Williams M, Gibbons G (2015) Design and manufacture of high performance hollow engine valves by additive layer manufacturing. Mater Des 69:44–55

9. Kobryn P, Semiatin S (2001) The laser additive manufacture of Ti-6Al-4V. JOM J Miner Met Mater Soc 53(9):40–42

10. Sterling AJ, Torries B, Shamsaei N, Thompson SM, Seely DW (2016) Fatigue behavior and failure mechanisms of direct laser deposited Ti–6Al–4V. Mater Sci Eng A 655:100–112

11. Liu QC, Elambasseril J, Sun SJ, Leary M, Brandt M, Sharp PK (2014) The effect of manufacturing defects on the fatigue behaviour of Ti-6Al-4V specimens fabricated using selective laser melting. Adv Mater Res 891:1519–1524

12. Bandyopadhyay A, Krishna B, Xue W, Bose S (2009) Application of laser engineered

net shaping (LENS) to manufacture porous and functionally graded structures for load bearing implants. J Mater Sci Mater Med 20(1):29–34

13. Harrysson OL, Cansizoglu O, Marcellin-Little DJ, Cormier DR, West HA (2008) Direct metal fabrication of titanium implants with tailored materials and mechanical properties using electron beam melting technology. Mater Sci Eng C 28(3):366–373

14. Hazlehurst KB, Wang CJ, Stanford M (2014) An investigation into the flexural characteristics of functionally graded cobalt chrome femoral stems manufactured using selective laser melting. Mater Des 60:177–183

15. Murr L et al (2010) Next-generation biomedical implants using additive manufacturing of complex, cellular and functional mesh arrays. Philos Trans R Soc Lond A 368(1917):1999–2032

16. Leong K, Cheah C, Chua C (2003) Solid freeform fabrication of three-dimensional scaffolds for engineering replacement tissues and organs. Biomaterials 24(13):2363–2378

17. Min B-M, Lee G, Kim SH, Nam YS, Lee TS, Park WH (2004) Electrospinning of silk fibroin nanofibers and its effect on the adhesion and spreading of normal human keratinocytes and fibroblasts in vitro. Biomaterials 25(7):1289–1297

18. Spoerke ED, Murray NG, Li H, Brinson LC, Dunand DC, Stupp SI (2005) A bioactive titanium foam scaffold for bone repair. Acta Biomater 1(5):523–533

19. Morlock M, Schneider E, Bluhm A, Vollmer M, Bergmann G, Müller V, Honl M (2001) Duration and frequency of every day activities in total hip patients. J Biomech 34(7):873–881

20. Ahmadi SM et al (2015) Additively manufactured open-cell porous biomaterials made from six different space-filling unit cells: the mechanical and morphological properties. Materials 8(4):1871–1896

21. Lütjering G (1998) Influence of processing on microstructure and mechanical properties of (α + β) titanium alloys. Mater Sci Eng A 243(1):32–45

22. Hanzl P, Zetek M, Bakša T, Kroupa T (2015) The influence of processing parameters on the mechanical properties of SLM parts. Proc Eng 100:1405–1413

23. Santos E, Osakada K, Shiomi M, Kitamura Y, Abe F (2004)Microstructure and mechanical properties of pure titanium models fabricated by selective laser melting. Proc Inst Mech Eng C J Mech Eng Sci 218(7):711–719

24. Kruth J-P, Levy G, Klocke F, Childs T (2007) Consolidation phenomena in laser and powder-bed based layered manufacturing. CIRP Ann Manuf Technol 56(2):730–759

25. Sercombe T, Jones N, Day R, Kop A (2008) Heat treatment of Ti-6Al-7Nb components produced by selective laser melting. Rapid Prototyp J 14(5):300–304